

Interpolation of mountain weather forecasts by machine learning

Kazuma Iwase and Tomoyuki Takenawa

Graduate School of Marine Science and Technology, Tokyo
University of Marine Science and Technology, 2-1-6 Etchujima,
Koto-ku Tokyo, 135-8533, Japan

Abstract

Recent advancements in numerical simulation methods based on physical models have enhanced the accuracy of weather forecasts. However, the precision diminishes in complex terrains like mountainous regions due to the several kilometers square grid used in numerical simulations. While statistical machine learning has also significantly advanced, its direct application is difficult to utilize physics knowledge. This paper proposes a method that employs machine learning to “interpolate” future weather in mountainous regions using current observed data and forecast data from surrounding plains. Generally, weather prediction relies on numerical simulations, so this approach can be considered a hybrid method that indirectly merges numerical simulation and machine learning. The use of binary cross-entropy in precipitation prediction is also examined.

1 Introduction

The rising interest in leisure activities, drone transportation to remote areas, and enhanced on-site operations efficiency have increased the demand for precise and comprehensive weather forecasting in mountainous regions. Recent advancements in numerical simulation methods, like NWP (Numerical Weather Prediction), have improved weather forecast accuracy. However, the precision diminishes in complex terrains like mountainous regions due to the several kilometers square grid used in numerical simulations. While statistical machine learning has also significantly advanced, its direct application is difficult to utilize physics knowledge.

In this paper, we propose a method that employs machine learning to “interpolate” future weather in mountainous regions using current observed data and forecast data from surrounding plains. Specifically, we predict the temperature and precipitation in Mt. Fuji and Hakone respectively, which are located in mountainous areas of the Kanto region in Japan, which is characterized by a

warm and humid climate. These predictions are made for 2, 7, 8, and 9 hours ahead. We then compare the accuracy of various machine learning models and existing weather forecast services.

Generally, weather prediction relies on numerical simulations, so this approach can be considered a hybrid method that indirectly merges numerical simulation and machine learning. Additionally, compared to directly using the results of numerical simulations, this approach is more accessible to general users as it utilizes past observed data and forecast data from weather services, which are readily available.

Furthermore, we examine the effectiveness of using a linear combination of root mean square error (RMSE) and binary cross-entropy as a loss function, given that precipitation values are non-negative and the occurrence of rainfall is significant.

2 Related works

Machine learning models used in weather forecasting can be divided into two categories: time series models that take a sequence of data with a specific temporal structure as input, and general regression models that do not require such structured input data. In time series models, it is common to use Recurrent Neural Networks (RNN), Long Short-Term Memory (LSTM), Convolutional Neural Networks (CNN), and their variants [9, 11, 13] (or see references in [2]). However, recently, a time series model based on Self-Attention called Tensorized Encoder Transformer (TENT) has been proposed, which has been reported to outperform RNN and LSTM in terms of accuracy [2]. On the other hand, in general regression models, ARIMA models and conventional neural networks (such as Multilayer Perceptrons) are used in studies such as [4] and [7]. In [10], an improved accuracy and consistency of short-term precipitation prediction are achieved by using Generative Adversarial Networks. For wind speed prediction, an improvement in accuracy has been demonstrated using Multistream Graph Attention Networks [5]. All these methods utilize observed data as model inputs. Similar to this paper, [12] uses a machine learning technique, Support Vector Machine (SVM), to interpolate numerical simulation results from Numerical Weather Prediction (NWP).

Regarding precipitation prediction, the study proposed in [8] uses binary categorical loss functions, employing an original loss function based on binary classification problem metrics. However, in this paper, we use a linear combination of binary cross-entropy and RMSE as a loss function.

3 Method

In this paper, we utilize not only the observed data up to the present but also future forecast data from the surrounding areas of the target location. While using future data might seem like data leakage, it is not an issue as the forecast

data from neighboring regions is available at prediction time. However, we do not use forecast data for mountainous regions, including the target location, as we assume that forecast data for mountainous regions have low reliability.

Due to the formal and qualitative differences in the data before and after the current point, this paper does not employ time series models. Instead, it employs regression models such as Linear model (Elastic Net), LightGBM [6], XGBoost [3], Random Forest (Extra Trees), and Neural Networks (NN, Multi Perceptron). Except for NN, these regression models are not expected to automatically extract features, and since some improvement in accuracy can be expected for NN as well, lag features and moving averages, which are variables commonly used in time series analysis, are used as input features.

Furthermore, the regression models other than NN are faster than deep learning-based time series models, enabling efficient training, inference, feature selection, and tuning in shorter time.

4 Experiments

4.1 Data

The experiment aims to predict the temperature at Mt. Fuji’s summit (elevation 3,775m) and precipitation at Hakone (elevation 855m), which are among a few mountain meteorological data stably provided by the Japan Meteorological Agency. Mt. Fuji is the highest peak in Japan, and meteorological observations including temperature, pressure, and humidity are recorded by the agency. Hakone is a complex volcano located approximately 30-40km southeast of Mt. Fuji, with the interior of the outer rim forming a highland. The observation point of the agency is situated at the foot of the central crater cone within the outer rim, where only precipitation is measured.

The surrounding areas include Odawara (temperature, precipitation, wind speed), Kawaguchiko (temperature, wind speed), Gotemba (temperature, precipitation, wind speed), Yamanakako (temperature, precipitation, wind speed), Nambu (temperature, precipitation, wind speed), and Fuji (temperature, precipitation, wind speed) (Fig. 1).

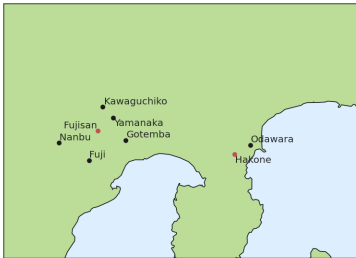


Figure 1: Observation points

Observation data were collected from the Japan Meteorological Agency (<https://www.data.jma.go.jp/risk/obsdl/index.php>), consisting of hourly observations for all variables from May 13, 2019, 01:00:00, to March 8, 2023, 00:00:00. The hourly forecast data for the surrounding areas were obtained through web scraping from “Weathernews” (<https://weathernews.jp/>) at 7 a.m. in Japan time from October 16, 2022, to March 8, 2023, comprising 144 days. Furthermore, to validate the prediction accuracy, hourly forecast data for the temperature at Mt. Fuji and precipitation in Hakone from Weathernews were collected at the same time during the same period, along with hourly forecast data for the elevations of 3,100m and 4,400m at Mt. Fuji from “Tenki to Kurasu” (<https://tenkura.n-kishou.co.jp/tk/>).

Table 1 presents the accuracy (RMSE) of the forecast data. It is evident that the temperature at Mt. Fuji exhibits a significantly larger RMSE compared to the surrounding areas, while the precipitation in Hakone does not show a substantial difference.

Table 1: RMSE of Forecasting

	Temperature		Precipitation	
	2 hours	8 hours	2 hours	8 hours
Fuji	0.866	1.595	1.033	0.613
Gotenba	1.246	1.294	0.684	0.303
Odawara	1.362	1.386	0.393	0.314
Yanamaka	1.466	1.192	0.972	0.348
Mt. Fuji	7.312	4.851	-	-
Hakone	-	-	0.613	0.314
Tenki (3775m)	4.296	3.627		

Tenki (3775m) is the weighted average of “Tenki to Kurasu” of 3100m and of 4400m.

In this experiment, during the test phase, forecast data for the surrounding area is obtained at 7:00 a.m., and then predictions for several hours into the future are made and compared with actual observed and forecast data. However, during the training phase, only observed data is used. In other words, the future forecast data is replaced with observed data for training, as it was not feasible to collect forecast data for the entire training period (approximately 3 years).

Data preprocessing includes removing data with missing values and missing value imputation. Subsequently, feature engineering is performed. In this experiment, when predicting the temperature at Mt. Fuji 8 hours ahead, the following data is used with 8 hours ahead as the reference point, i.e. “8 hours ago” in the following implies the time of making prediction:

- (i) The time of a day and the day of a year represented as sin, cos functions, which have cycles corresponding to the hours in a day and the days in a year.
- (ii) The surrounding areas and the target locations: Observed values from 8,

9, 10, 23, 24, and 25 hours ago; Differences in observed values between 8, 9, and 24 hours ago and their respective values from 1 hour before; The differences between the observed values from 8 hours ago and those from 24 hours ago and 7 days ago

- (iii) The surrounding areas only: For temperature at Mt Fuji: Forecast values (replaced by observed values during training) for 0, 1, 2, 3, 4 hours ago; The differences between the forecast values (observed values during training) for 0, 1, 2 hours ago and their respective values from 1 hour earlier
- (iv) The target locations only: The average, maximum, and minimum values over the past 24 hours and 7 days starting from 8 hours ago

In predicting precipitation in Hakone 8 hours ahead, we utilize the data employed for temperature prediction but excluding the data of (i) corresponds to the time of day; excluding all the data of (ii); (iii) is replaced by forecast values (replaced by observed values during training) for 0, 1, 2, 3, 4, 5 and differences between 0, 1, 2, 3, 4 hours ago and 1 hour earlier; adding to (iv) the average, maximum, and minimum values over the past 12 hours starting from 8 hours ago.

The data used for predicting whether 7 or 9 hours ahead is almost similar to the 8 hours case and we omit the detail.

In predicting temperature at Mt. Fuji 2 hours ahead, the following data are used with the reference point set to 2 hours ahead.

- (i) The time of a day and the day of a year represented as sin, cos functions
- (ii) The surrounding areas and the target locations: Observation values from 2, 3, 4, and 5 hours ago; the differences between observed values from 2, 3 hours ago and their respective values from 1 hour before
- (iii) The surrounding areas only: The forecast values (observed values during training) from 0 and 1 hour ago; the differences between the forecast values (observed values during training) from 0 hour ago and 1 hour ago
- (iv) The target locations only: The average, maximum, and minimum values of the past 24 hours and the past 7 days, starting from 2 hours ago

In predicting precipitation in Hakone 2 hours ahead, the time of day is not used in the data of temperature prediction (i), and instead, the average, maximum, and minimum values of the past 12 hours starting from 2 hours ago are added to (iv).

During the tuning of hyperparameters, the time-series data divided for cross-validation is used, while during testing, the model trained with all the available training data is used (Table 2). It should be noted that although the three validation datasets combined cover one year, the test data covers a period of 144 days centered around the winter season, which may lead to data bias.

Table 2: Number of time periods

Data	Train	Validation / test
Fold1	20057	2920 (2021/10/16–2022/02/14)
Fold2	22977	2920 (2022/02/14–2022/06/16)
Fold3	25897	2920 (2022/06/16–2022/10/15)
Test Data	28817	144 (2022/10/16–2023/03/08)

4.2 Results

4.2.1 Comparison of model accuracy and training time

The linear model with L1 and L2 regularization (Elastic Net), LightGBM, XGBoost, Random Forest (Extremely Randomized Trees), and NN (with architecture Dense(1000, ReLU) - Dense(1000, ReLU) - Dense(100, ReLU) - Dropout(ratio=0.2) - Dense(1)) were compared through cross-validation on the training data. Their hyperparameters were tuned using Optuna[1] or manual tuning.

Table 3 presents the results of models, comparing the RMSE (Root Mean Squared Error) and the training time (for the hyperparameter-tuned models).

LightGBM and XGBoost demonstrated superior performance in terms of RMSE (as these two models are quite similar). NN required a longer training duration, while Elastic Net, LightGBM, and XGBoost necessitated shorter training durations. It is commonly accepted that LightGBM is faster than XGBoost, although training durations can fluctuate. Furthermore, the number of iterations derived from early stopping during the model tuning process was used for training on the entire training data. Hence, depending on the tuning results, the number of iterations may vary, and XGBoost could have a shorter training duration.

4.2.2 Feature Extraction

For feature extraction, we used LightGBM, which consistently demonstrated high performance in terms of accuracy and training time in the experiments described in Section 4.2.1.

After parameter tuning, we selected 70 features for temperature prediction and 30 features for precipitation prediction based on their importance in the trained LightGBM models (Fig. 2). The importance of a feature is determined by counting how many times it was used for branching in the decision trees of the LightGBM algorithm. However, for the features related to time and date represented by sin and cos, we adopted them regardless of their importance score.

By performing feature extraction, we expected to reduce the inference time after training and mitigate overfitting. Comparing the RMSE on the test data between LightGBM trained with all the features (LGBM all) and LightGBM trained with only the extracted features (LGBM top 30/70), as shown in Table

Table 3: RMSE and training times of Models

	Temperature at Fujisan		Precipitation at Hakone	
	2 hours	8 hours	2 hours	8 hours
Elastic Net	1.178	2.188	1.063	1.093
	1.636	4.937	0.130	0.134
LightGBM	1.109	2.006	0.951	0.999
	0.890	2.022	1.333	0.304
XGBoost	1.129	2.078	0.932	0.998
	0.921	2.090	0.560	0.267
Extra Trees	1.140	2.101	1.024	1.085
	10.802	23.481	10.764	11.665
Neural Net	1.207	2.119	0.992	1.079
	63.634	60.806	54.931	35.162

The upper and lower numbers are the averages of RMSE on **the 3 Validation Datasets** and training times on **the Test Datasets** respectively.

5, we observed similar or slightly improved accuracy with the extracted features.

From Fig. 2, we can see that past temperatures at Mt. Fuji are important for temperature prediction, while surrounding precipitation around the target time is crucial for precipitation prediction in Hakone.

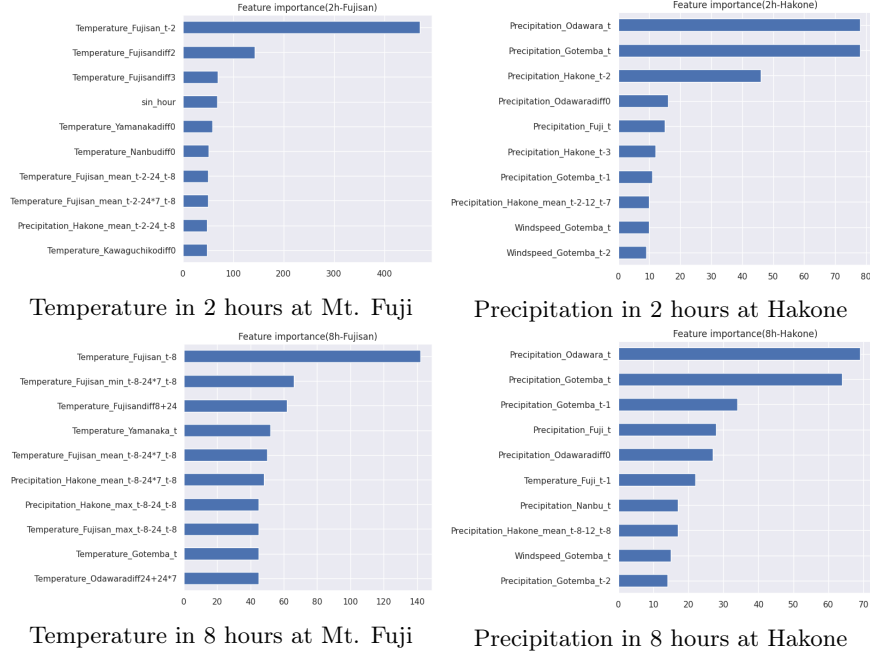


Figure 2: Top 10 feature importance of LightGBM

4.2.3 Loss function using binary cross-entropy

The observed precipitation data used in this experiment take non-negative values with a resolution of 0.5 mm. From users' perspective, it is important to determine whether the precipitation is exactly 0 mm, or 0.5 mm or higher. In order to incorporate it into the learning, we use a linear combination of the RMSE loss and the shifted binary cross entropy as follows.

Let y and \hat{y} be the observed value (ground truth) and predicted value of precipitation respectively and let z and \hat{z} be the binarized value with a threshold of 0.25 for y and the value of a shifted sigmoid function at \hat{y} respectively as

$$z = \begin{cases} 1 & (\text{as } y \geq 0.25) \\ 0 & (\text{as } y < 0.25) \end{cases} \quad (1)$$

$$\hat{z} = \frac{1}{1 + e^{-a(\hat{y}-0.25)}}, \quad (2)$$

we define L_{binary} as a binary cross-entropy of \hat{z} for z :

$$L_{\text{binary}} = -z \log \hat{z} - (1 - z) \log(1 - \hat{z}) \quad (3)$$

and L as its linear combination with the RMSE loss:

$$L = \alpha \text{RMSE}(y, \hat{y}) + (1 - \alpha) L_{\text{binary}}. \quad (4)$$

where $\alpha \geq 0$ is a constant.

We compared the results of training with standard RMSE loss (i.e., L with $\alpha = 1.0$) and the above L with positive α , using RMSE as the evaluation metric (Table 4 and Table 5). Specifically, we set as $a = 16$, $\alpha = 0.7$ for the latter. This value was determined through experimentation to optimize the influence of binary cross-entropy while preserving acceptable accuracy on the validation data. Regarding the validation data (Table 4), LGBM (all/top 30) showed similar or slightly better performance than LGBM binary (all/top 30). On the other hand, for the test data (Table 5), LGBM binary (all/top 30) achieved superior performance in most cases than LGBM (all/top 30).

Note that the graph of the loss function, as shown in Fig. 3, indicates that L_{binary} emphasizes whether \hat{y} is greater than 0.25 in comparison to RMSE. When using L_{binary} , we also used it as the evaluation metric for the tuning by Optuna. The relationship between L_{binary} and RMSE during the tuning process is depicted in Fig. 4. The values of L_{binary} and RMSE generally correlate, demonstrating that as L_{binary} decreases, RMSE tends to decrease as well.

Table 4: RMSE losses of precipitation prediction in Hakone on the Validation data sets

Model	2 hours	7 hours	8 hours	9 hours
LGBM (all)	0.953	0.987	0.994	0.988
LGBM (top 30)	0.934	0.984	0.986	0.978
LGBM binary (all)	0.981	0.987	0.995	0.993
LGBM binary (top 30)	0.947	0.995	1.000	0.995

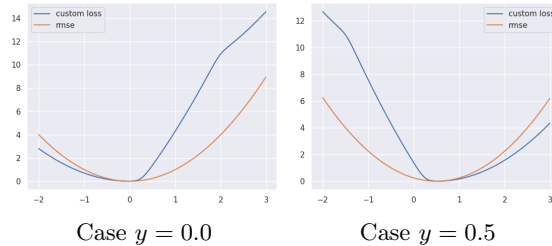


Figure 3: Graphs of RMSE and L_{binary} for $y = 0.0$ and $y = 0.5$

Horizontal axis: \hat{y} , Vertical axis: losses. The blue curves represent the L_{binary} losses with $a = 16$, $\alpha = 0.7$, while the orange curves represent the RMSE losses.

Table 5: RMSE losses of predictions/forecasts on the Test data sets

Feature at Station	Model and Forecast	2 hours	7 hours	8 hours	9 hours
Temperature at Fujisan	LGBM (all)	1.068	1.944	2.015	2.242
	LGBM (top 70)	1.058	1.944	2.155	2.215
	LGBM (no future)	1.112	2.144	2.286	2.488
	Weathernews	7.133	5.279	4.852	3.902
	Tenki (3100m)	7.154	-	6.260	-
	Tenki (4400m)	2.869	-	2.778	-
Precipitation at Hakone	Tenki (3775m)	4.296	-	3.627	-
	LGBM (all)	1.589	0.501	0.440	0.656
	LGBM (top 30)	1.161	0.444	0.463	0.643
	LGBM binary (all)	1.195	0.440	0.382	0.609
	LGBM binary (top 30)	1.167	0.353	0.379	0.579
	LGBM binary (no future)	0.747	0.604	0.793	0.895
	Weathernews	1.457	0.344	0.443	0.619

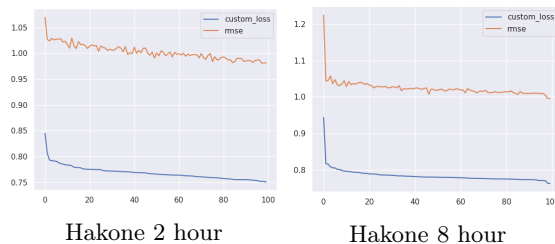


Figure 4: Comparison of the RMSE and the L_{binary} losses during tuning for all features by Optuna

Horizontal axis: Learning number, Vertical axis: losses. The data is sorted by L_{binary} .

4.2.4 Comparison of LightGBM with weather forecasting services

We compared the predicted temperature values at Mt. Fuji and precipitation values in Hakone for 2 hours, 7 hours, 8 hours, and 9 hours ahead with the observed data, the forecasts from Weather News, and the forecasts from Tenki to Kurasu (Table 5). Additionally, we created a model called LightGBM (no future), which uses only the observed data without incorporating any forecast data, to examine the impact of using forecast data.

In the prediction of temperature at Mt. Fuji for the Test data, LightGBM significantly outperformed the forecast services for all time points. Particularly, the accuracy of LGBM (all/top 70) was high for the predictions at 7, 8, and 9 hours ahead.

For the prediction of precipitation in Hakone for the Test data, LightGBM (no future), which used only the observed data, achieved the highest accuracy for the 2-hour ahead prediction, while LightGBM using binary cross-entropy showed higher accuracy for the predictions at 7, 8, and 9 hours ahead.

Furthermore, it should be noted that the accuracy for the predictions at 7, 8, 9 hours ahead is higher than that for the 2-hour ahead prediction for precipitation in Hakone. This discrepancy is attributed to the limited size of the Test data (144 data), which made it more susceptible to the influence of outliers such as 15.0 [mm] at 9 A.M. on 2023-02-19 (Fig. 5).

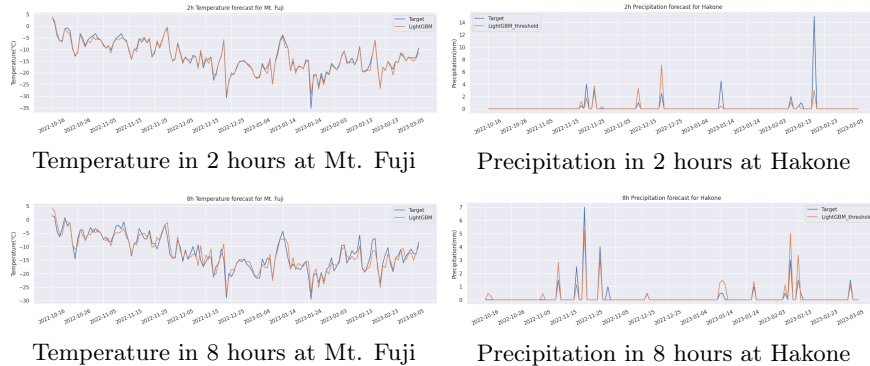


Figure 5: Prediction in time series

5 Conclusion

The experiments in this paper aimed to predict weather in mountainous areas by interpolating forecasts for the surrounding regions. The gradient boosting decision tree model performed superior in terms of both accuracy and learning speed. Moreover, the accuracy of test data was enhanced by selecting and restricting the input features. In predicting precipitation, the use of a linear sum of RMSE and shifted binary cross entropy as the loss function improved the accuracy of the test data.

Our method outperformed some existing weather services in predicting the temperature at Mt. Fuji. However, no improvement was observed in predicting precipitation at Hakone 7, 8, and 9 hours ahead of time. This could be attributed to the comparable accuracy of the precipitation forecast for Hakone and the surrounding areas.

Due to the difficulty in obtaining long-term forecast data, observed data were used instead of forecast data for the surrounding areas in the future during the training phases in this experiment. If stable long-term forecast data, without significant algorithmic changes, becomes available, it would be more appropriate for training. While it is believed that a more versatile model could be created by directly using the NWP numerical data, this does not imply that the methods

in this study can be immediately applied, given the higher dimensionality of the input data.

Declarations

Funding KI was supported by the WISE Program for the Development of AI Professionals in the Marine Industry at TUMSAT. TT was supported by the Japan Society for the Promotion of Science, Grand-in-Aid (C) (22K03383).

Conflict of Interest All authors certify that they have no affiliations with or involvement in any organization or entity with any financial interest or non-financial interest in the subject matter or materials discussed in this manuscript.

Data and Code Availability Available from <https://github.com/KazumaIwase/Interpolation-of-mountain-weather-forecasts-> where the forecast data by “Weathernews” or “Tenki to Kurasu” has been replaced with artificially created dummy data.

Author Contributions KI collected data, developed codes and drafted the manuscript. TT planned the research, revised the codes and edited the manuscript.

References

- [1] Akiba T., Sano S., Yanase T., Ohta T., Koyama M., Optuna: a next-generation hyperparameter optimization framework, In *KDD '19: Proceedings of the 25th ACM SIGKDD International Conference on Knowledge Discovery & Data Mining* July 2623–2631 (2019) .
- [2] Bilgin, O., Mağa, P., Vergutz, T., Mehrkanoon, S., TENT: Tensorized Encoder Transformer for Temperature Forecasting, *arXiv preprint arXiv:2106.14742*, (2021).
- [3] Chen T., Guestrin C., XGBoost: A Scalable Tree Boosting System, In *Proceedings of the 22Nd ACM SIGKDD International Conference on Knowledge Discovery and Data Mining* 785–794 (2016) .
- [4] Chen L., Lai X., Comparison between arima and ann models used in short-term wind speed forecasting, In *2011 Asia-Pacific Power and Energy Engineering Conference, IEEE* 1–4 (2011).
- [5] Dogan A., Siamak M., Multistream Graph Attention Networks for Wind Speed Forecasting, *arXiv preprint arXiv:2108.07063*, (2021).
- [6] Ke G., Meng Q., Finley T., Wang T., Chen W., Ma W., Ye Q., Liu T-Y., LightGBM: A Highly Efficient Gradient Boosting Decision Tree, In *Advances in Neural Information Processing Systems* **30** 3146–3154 (2017).

- [7] Kuligowski, R. J., Barros, A. P., Localized precipitation forecasts from a numerical weather prediction model using artificial neural networks, *Weather and forecasting* **13** (4) 1194–1204 (1998).
- [8] Larraondo, P. R., Renzullo, L. J. , Van Dijk, A. I. J. M., Inza, I., Lozano, J. A., Optimization of deep learning precipitation models using categorical binary metrics, *Journal of Advances in Modeling Earth Systems* **12** (5) 10.1029/2019MS001909 10pp (2020).
- [9] Mehrkanoon, S., Deep shared representation learning for weather elements forecasting, *Knowledge-Based Systems* **179** 120–128 (2019) .
- [10] Ravuri S., Lenc K., Willson M., Kangin D., Lam R., Mirowski P., Fitzsimons M., Athanassiadou M., Kashem S., Madge S. et al., Skilful precipitation nowcasting using deep generative models of radar, *Nature* **597** 672–677 (2021).
- [11] Shi, X., Chen, Z., Wang, H., Yeung, D.-Y., Wong, W., Woo, W., Convolutional LSTM Network: A Machine Learning Approach for Precipitation Nowcasting, In *Advances in Neural Information Processing Systems* **28** (2015).
- [12] Yoshikane, T., Yoshimura, K., Development of method of spot weather forecast using machine learning, In *Proceedings of the Annual Conference of JSAI* **33** (2019).
- [13] Zaytar, M. A., El Amrani, C. Sequence to sequence weather forecasting with long short term memory recurrent neural networks. *Int. J. Comput. Appl.* **143** 7–11 (2016).